Maejo Int. J. Sci. Technol. **2014**, *8*(02), 165-180

Maejo International Journal of Science and Technology

ISSN 1905-7873
Available online at www.mijst.mju.ac.th

Full Paper

Spring-based tactile array for assistive robotic surgical applications

Safar Pourabbas [1] and Sunita Chauhan [2, *]

[1] Department of Industrial Design, Applied Art School, Tabriz Islamic Art University, Iran
[2] School of Mechanical and Aerospace Engineering, Monash University, Australia

* Corresponding author, e-mail: sunita.chauhan@monash.edu

Received: 27 May 2013 / Accepted: 16 June 2014 / Published: 27 June 2014

Abstract: Tactile sensing is highly desirable for robotic surgery, more specifically minimally invasive surgery, during tissue/organ manipulation. For safe handling and safe grasping of tissues, the two most important aspects are the monitoring and controlling of force and the stiffness information that exists at the sensor-tissue interface. In this study, a spring-based tactile sensing system is used to measure both the interacting forces and stiffness in surgical assistive applications. A differential analysis is performed to obtain the stiffness of a compliant object whilst individual elements of the proposed sensing array experience different deflections when they come in contact with the object. A lumped model formulation for tactile array performance shows that larger differences in stiffness between the force sensing elements provide higher sensitivity in evaluating the object stiffness. For benchmarking of our sensing principle, a macro tactile-sensor array is designed and tested. Different stiffness combinations of the sensing elements show an inverse linear relationship between the stiffness of the object and the output signal magnitude of the stiffness sensing unit. The proposed tactile array based on spring-based stiffness sensing has high potential for safe grasping/handling of the tissues when integrated into the jaws of a surgical grasper during the minimally invasive robotic procedures.

Keywords: tactile sensor, minimally invasive surgery, force sensing, stiffness sensing

INTRODUCTION

Tactile sensing is highly desirable for minimally invasive surgery (MIS) in order to overcome severe reduction in the surgeons' sensory perception during organ/tissue manipulation. Thus, the integration of tactile sensors into surgical instruments has drawn researchers' attention [1, 2]. The

application of a tactile sensing system to the MIS can be categorised as either diagnostic or assistive. Diagnostic tactile systems involve examining dynamically changing tissue characteristics, such as hardness/softness and elasticity, to evaluate abnormal structures and diseased areas. Most of the studies conducted in diagnostic tactile sensing originate from a single sensing principle of resonant vibrations [3-8]. A resonant vibrating sensor consists of two lead zirconate titanate elements, one as a transducer and the other for vibration pickup. Normally, a rod that comes in contact with the tissue is used as a 'feeler' that vibrates at the resonance frequency of the sensor. As a result, the resonance frequency of the sensor-tissue pair changes to a new value and is detected by a phase-shift circuit to be interpreted as a measure of tissue stiffness. Thus, in general, the diagnostic tactile sensing systems using the resonant vibration sensing principle are based on a non-force approach.

An assistive tactile sensing, on the other hand, is aimed for safe grasping and handling of tissues during surgical interventions. Thus, the sensing of grasping and pulling forces during tissue manipulation plays a key role in fulfilling such an objective, and the measured force may be regarded as the most important parameter in the assistive tactile systems for MIS. Initial attempts on assistive tactile feedback were based on the integration of the force sensing elements into the forceps of surgical grasping instruments [9,10]. While measurement of the forces present at the grasper-tissue interface is necessary, it is not sufficient to secure the safe handling of tissues. In this aspect, stiffness sensing can be considered the most favourable parameter since it can represent the firmness of grasping at the tissue-grasper interface. Integrating force and stiffness together would thus result in the safe grasping and handling of tissues.

Attempts on simultaneous sensing of force and stiffness can be categorised as active and passive procedures. Takao et al. [11] developed a multifunctional tactile imager using active sensing approach. For elasticity detection of object, they applied a vibration component to assess the swelling pressure of the sensor skin. Shikida et al. [12] developed a piezo-resistive tactile sensor equipped with a chamber for pneumatic actuation. In these active procedures, besides signal read-out wiring, it was also necessary to supply pressurised air into the sensing site. This requirement adds to the space restriction problem while integrating the tactile sensing arrays into the surgery graspers.

A passive spring-based stiffness sensing approach employs two force sensing elements with different stiffness values in a parallel fashion. When these elements come in contact with a compliant object, they experience different deflections which can be formulated to obtain the stiffness of the object. By making use of such a force-based approach, both the stiffness and forces present at the grasper-tissue interface can be measured simultaneously. Engel et al. [13, 14] developed a multimodal polymer-based sensor skin of which stiffness sensing, as one of the sensing modes, takes benefit of the spring-based principle. The study mainly focused on the multimodality of the sensor skin and had not concentrated in exploring the effectiveness of this principle in accurate evaluation of object stiffness and its applicability to different engineering fields, especially in MIS. Peng et al. [16] developed a spring-based stiffness sensor using micro-electro-mechanical systems (MEMS) technology. They reported measurement results for three different polymers while emphasising only on the fabrication aspects of MEMS capacitive sensors. Dargahi et al. [15] used the stiffness sensing principle for tissue softness measurement. In their study, they made use of polyvinylidene difluoride (which is only suited for dynamic response) instead of strain gauges as the sensing element. However, static and quasi-static responses are equally important as dynamic ones. Thus, for evaluating the effectiveness of assistive tactile sensing based on spring-based stiffness sensing, it is

Maejo Int. J. Sci. Technol. **2014**, *8*(02), 165-180

favourable to use strain gauges as sensing elements. In short, the application of spring-based stiffness sensing to tactile sensing needs a further focused study for targeted MIS applications.

The next important criterion is the optimum positioning of sensors on desired surgical instruments. They can be placed or integrated at various possible locations on a surgical manipulator, such as near the actuation mechanism, on the manipulator shaft and into the grasper. Integrating the sensing elements into the grasper of a surgical manipulator provides the most direct measurement of forces. This is because friction and other disturbances generated from any moving mechanisms do not affect the measurement of sensed data while it could happen at other locations within a surgical system. However, the jaws of the grasper have severe space limitation, which makes the integration very challenging [1]. This requires some micro-fabrication technology for high-resolution sensing arrays while maintaining the magnitude and sensitivity of the desired data. There have been several attempts on the fabrication of force and pressure sensing arrays using MEMS fabrication techniques for applications other than in MIS. For instance, piezo-resistive sensor arrays comprising three axial force sensors with sub-millimetre resolution can be realised [17-20]. Further studies were conducted on understanding the issues of miniaturisation of the sensing arrays as well as various technologies and transduction methods used to improve the tactile sensing capabilities [21, 22]. Such high resolution micro-sensors are desirable for MIS as they can be integrated into a surgical grasper. However, prior to miniaturising, it is necessary to investigate and validate the sensing concept and its effectiveness in evaluating the stiffness of biological objects, along with other determining factors for a specified performance.

In this paper, a spring-based stiffness sensor array for simultaneous sensing of both the grasping force and the object stiffness is investigated. A lumped model is used for the formulation and description of the sensing concept. By making use of a macro tactile array as benchmark, the experimental validation of the sensor design is reported. Also, a detailed analysis of the tactile array fabrication technique and its performance is presented.

SENSOR DESIGN CONCEPT AND FORMULATION

The spring-based stiffness sensing concept is illustrated in Figure 1(a), in which each stiffness sensing unit is represented by a pair of force sensing elements (with different stiffness). These force sensing elements are named as measuring sensing element and reference sensing element with K_m and K_r as their stiffness values respectively. The measured stiffness, K_m, is designed to be smaller than the reference stiffness, K_r, and hence the measuring sensing element experiences higher deflections as compared to the reference element. K_{obj} represents the stiffness of a compliant object to be measured. When a stiffness sensing unit (comprising a pair of measuring and reference sensing elements) is driven either manually or by motor, against an object with stiffness K_{obj}, the measuring and reference sensing elements experience different deflections, represented as Δ-δ_m and Δ-δ_r respectively. The value of the ratio, $R = \Delta\text{-}\delta_m/\Delta\text{-}\delta_r$, is considered to be proportional to the stiffness of the object, K_{obj} [13,14]. This means that when a stiffness sensing unit with a given pair of K_m and K_r values comes in contact with objects with different stiffness, it should record different values for R. Thereby, a correlation between R and K_{obj} can be established and in this way the governing principle not only provides a possibility of measuring tactile forces, but also measures the stiffness of compliant objects. In this study a linear spring model is used to simulate the sensor-tissue interaction and simplify the sensing principle. However, the viscoelastic properties of tissues are not considered at this stage. Our

Maejo Int. J. Sci. Technol. **2014**, *8*(02), 165-180

assumption is supported by an experimental study of Rentschler et al. [23], who studied liver tissue stiffness and considered both the linear model and viscoelastic model in simulating the tissue behaviour. Their study suggests that a linear force-deflection relationship for liver tissue is adequate.

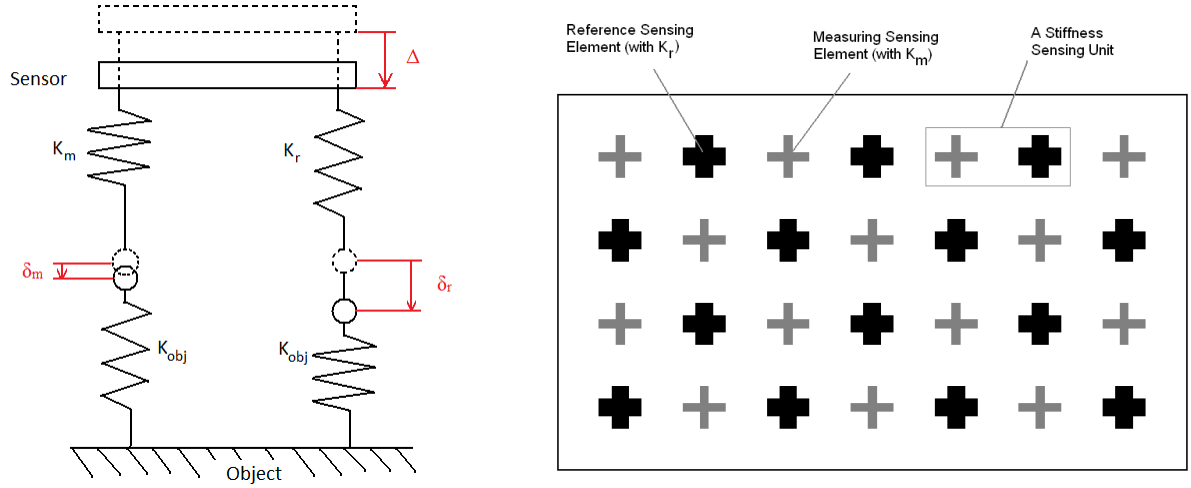

(a) (b)

Figure1. Sensor design concept: (a) a lumped model description of the interaction between a spring-based stiffness sensor and the object; (b) schematic presentation of the proposed force and stiffness tactile sensor array

The sensor prototype can be realised as an array of the force sensing elements with two different stiffness values which are arranged alternately as shown in Figure 1(b). In this Figure, the '+' patterns represent either the measuring or the reference force sensing element while a pair of one measuring and one reference sensing element is considered as a stiffness sensing unit. The force sensing elements, in general, measure the tri-axial forces. Such a sensing system can provide three components of forces as well as the contact stiffness, thereby rendering a four-component vector as its output. For formulating the performance of the proposed sensing array, the lumped model in Figure 1(a) is considered. When the sensor is given a displacement of Δ against the object, the interface between the sensing elements and object will experience δ_m and δ_r displacements for the measuring and reference sensing elements respectively. Thus, the deflections at the measuring and reference sensing elements can be expressed as Δ-δ_m and Δ-δ_r respectively. Based on the force equilibrium in the vertical direction, we can formulate the following relationship:

$$K_{obj}\delta_m = K_m(\Delta - \delta_m) \Rightarrow \quad \delta_m = \frac{K_m}{K_{obj} + K_m}\Delta$$
$$K_{obj}\delta_r = K_r(\Delta - \delta_r) \Rightarrow \quad \delta_r = \frac{K_r}{K_{obj} + K_r}\Delta \qquad (1)$$

Following (1), the ratio of data read by the measuring sensing element to that of the reference sensing element, $R = (\Delta\text{-}\delta_m)/(\Delta\text{-}\delta_r)$, can be related to the stiffness of sensing elements and object (stiffness-sensing-unit output) as follows:

Maejo Int. J. Sci. Technol. **2014**, *8*(02), 165-180

$$R = \frac{\Delta - \delta_m}{\Delta - \delta_r} = \frac{K_r + K_{obj}}{K_m + K_{obj}} \quad (2)$$

Thus, R is a function of stiffness of the object, K_{obj}, and also stiffness of the force sensing elements, K_m and K_r. Equation (2) can be rearranged in a way that K_{obj} can be explicitly expressed as a function of R while K_m and K_r are constant for a given sensor array:

$$K_{obj} = \frac{K_r - RK_m}{R - 1} \quad (3)$$

Further explanation and finite element method (FEM) analysis of the concept were reported in our earlier work [24], according to which sensor arrays with higher K_r/K_m ratios provide higher sensitivity. Also, it was concluded that a stiffness sensing unit with K_r and K_m higher than the object stiffness, K_{obj}, is required in order to obtain a higher sensitivity for object stiffness.

VALIDATION: MACRO-TACTILE SENSING ARRAY AS A BENCHMARK

This section concentrates on the experimental validation of sensor design concept including both the force measurement and the stiffness evaluation. For this purpose, a macro-tactile array was designed, fabricated, calibrated and tested.

Design of Macro-Tactile Array

The main element of this macro-tactile array is a flexural element as shown in Figure 2(a). In this design, strain gauges are installed at the flexing point of each sensing element. Following the application of an upward force at the tip of a given sensing element (contact area), the tip gets deflected, which is measured as a change in voltage across the poles of the corresponding strain gauge. For pairs of sensing elements with different stiffness, with each pair representing a stiffness sensing unit, the sensing elements are set to have different measuring arm lengths (i.e. $a1 \neq a2$ in Figure 2(a)). As a result, even though such design can only measure one component of the general force vector (the normal component), it can also sense the required stiffness. The macro-tactile array as shown in Figure 2(a), was designed as 2×5 array of sensing elements with a resolution of 4 mm. Sensing elements with longer arms are more compliant as compared to ones with shorter arms. This design was analysed using ANSYS®. Figure 2(b) illustrates an example of the meshed model for sensing elements. The model includes the applied force to the sensing element tip and boundary condition. A 2 N force was applied at the tip upwards while the thickness of the flexing point was made to vary from 0.15 mm to 0.4 mm. The sensor material was made of aluminum, with elastic modulus of 69000 MPa and poison ratio of 0.33. Planar stress condition with a model thickness of 3 mm was assumed. The flexing point arm length was varied from 4 mm to 8 mm. The deflection of the sensor tip and strain at the surface of the flexing point were obtained for all possible combinations. Based on the results, the sensing element with a flexing point of 0.25 mm in thickness was chosen for the sensor fabrication. In such sensing elements fabricated from an aluminum sheet of 3-mm thickness, the strain values for different arm lengths (as stated above) varied between 0.2711-0.6316%. Since the strain gauges are very sensitive devices, such a large range of strain is a considerable value to be measured.

Maejo Int. J. Sci. Technol. **2014**, *8*(02), 165-180

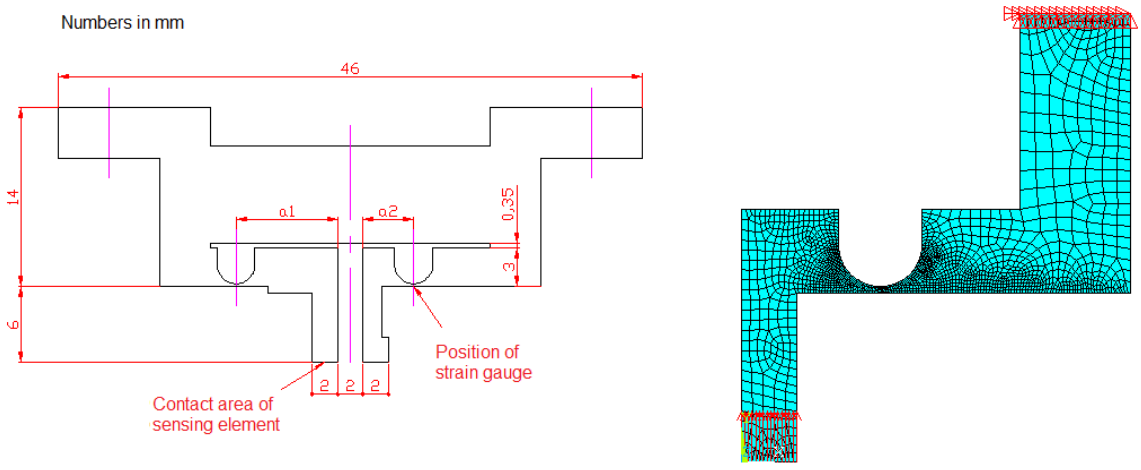

(a) (b)

Figure 2. Design of macro-tactile sensor: (a) side view of a pair of sensing elements with different measuring arms; (b) example of FEM modelling for the macro sensing element

Fabrication of Macro-Tactile Array

Following the FEM analysis of sensing elements, the detailed design of mechanical parts for the macro-tactile set-up was performed. The whole set-up as shown in Figure 3 consists of the sensing elements, along with the holding and clamping parts to fix them in an array. Each sensing element, Figure 3(a), was fabricated by a wire-cut process, resulting in a negligibly small cutting force and the cutting of flexing point in the sensing element being conducted easily. Figure 3(b) shows the overall assembled tactile set-up. It also shows the translational axes of the set-up which were used during the calibration of the sensing elements. Figure 3(c) depicts the completed macro-tactile sensing set-up following the bonding of strain gauges on the sensing elements, along with soldered electrical connections to the measuring circuit.

The amplification and read-out circuitry for the signals from individual sensing elements in the array is presented schematically in Figure 3(c). Each sensing element in the tactile array was set up in the form of a quarter-bridge configuration. Strain gauges of 120 Ω each were bonded on each sensing element beside three other reference strain gauges to form a Wheatstone bridge. A single MOSFET device was used to isolate the connection between the zero line of the power source and the ground. In this way the current flow into the strain gauges prior to read-out signals was prevented. Only at the read-out moment did a signal from a digital output of the DAQ device activate the MOSFET and the current flow into the zero line. The output voltages of the bridges were amplified by AD621 instrumentation amplifier and were acquired by the DAQ device (NI USB 6258) through Lab-View programme. For each of the sensing elements in the tactile array, the programme was set to take 10 samples in every measurement and provide their average as the representative value for that particular measurement.

Maejo Int. J. Sci. Technol. **2014**, *8*(02), 165-180

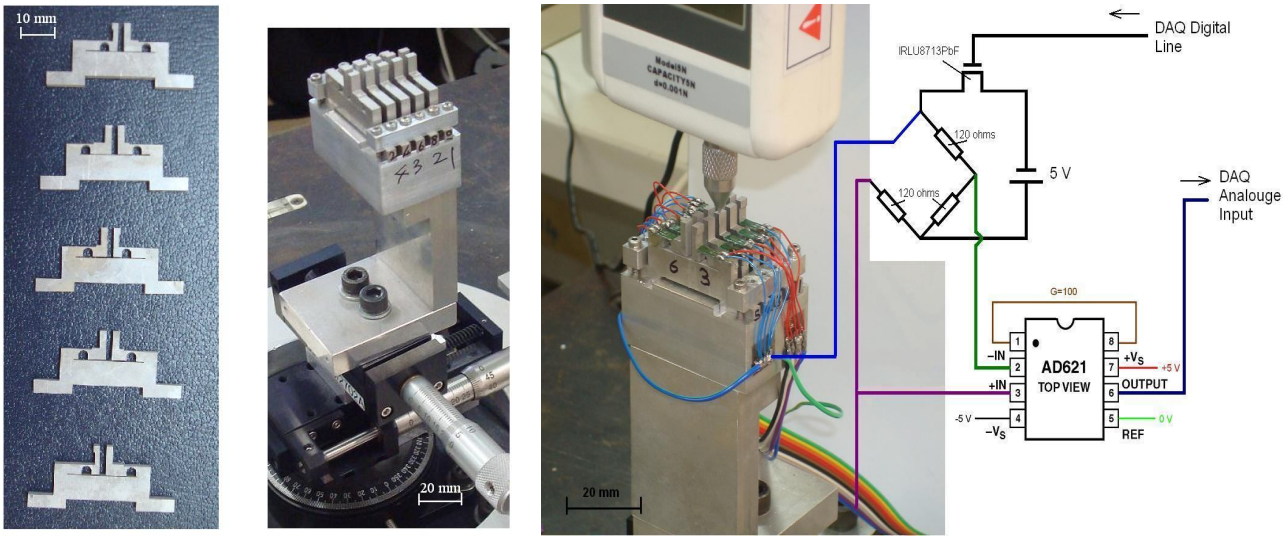

(a) (b) (c)

Figure 3. (a) Tactile sensing elements fabricated by wire-cut process; (b) The whole mechanical set-up after its fabrication and assembly; (c) Macro-tactile set-up after bonding of strain gauges on sensing elements and soldering of connection wires, together with schematic presentation of read-out circuit

Calibration of Macro-Tactile Array

A mechanical set-up using micro-stages for carrying the macro-tactile array was developed for calibration of the sensing elements (whose horizontal axes can be seen in Figure 3(b)). Each sensing element was positioned accurately below the commercial Sauter FH5 force sensor tip (Figure 3(c)). This force sensor itself was installed on the Z-axis and pointed downward. A differential Opto Sigma micro-meter head was installed on the Z-axis to give a 0.5-µm vertical resolution. The commercial force sensor had a maximum 5-N loading capacity and a 0.001-N resolution for measuring the forces. The calibration process was aimed to get both the force deflection relationship and the signal deflection relationship for each sensing element. The Z-axis carrying the commercial force sensor was displaced in increments of 25 µm to a total displacement of 150 µm. This was repeated for all the sensing elements. As the commercial force sensor utilises a stiffness-based load-cell with stiffness of 57.04 N/mm, a part of the applied 150-µm displacement was absorbed by the force sensor itself. By considering the commercial force sensor and the macro-sensing element as two springs in series, the deflection of each sensing element was offset by deducing the commercial force sensor deflection.

Figure 4 shows the calibration graphs for a typical sensing element. For a given sensing element, every measurement was conducted in triplicate and the collected data were averaged to obtain a representative graph. Figure 4(a) shows the applied force (N) versus sensing element deflection (µm). Hence the slope of the graph represents the stiffness of the sensing element, which amounts to 40.1 N/mm in this case. Figure 4(b) depicts a relationship between signal (V) and deflection (µm). As it can be seen, both force deflection and signal deflection exhibit a linear relationship. The resolution of the force measurement was equal to or above 0.01 N and the linearity error was in the range of 1.15-2.32 %.

Maejo Int. J. Sci. Technol. **2014**, *8*(02), 165-180

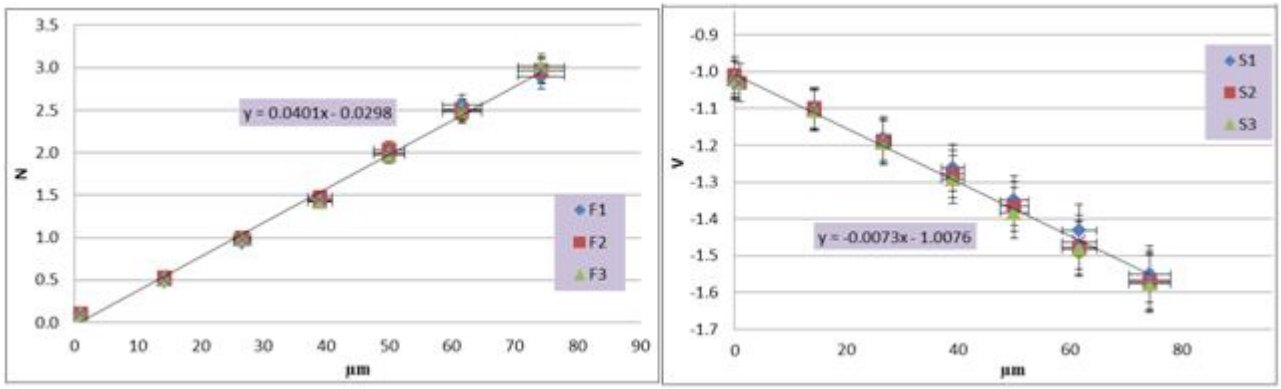

(a) (b)

Figure 4. Example of calibration graphs for sensing elements: (a) force (N) vs deflection (μm); (b) voltage change (V) vs deflection (μm)

Table 1 summarises the calibration results for all sensing elements (element no. 5 not functioning). From this Table, the deflection in each sensing element, Δ, can be calculated as:

$$\Delta = (1/K_v)*(V-V_0) \quad (4)$$

where K_v is the slope of the data represented in Figure 4(b) for any given sensing element, V_0 is the initial signal (zero deflection) and V is the measured signal in volts. Next, by computing the value for Δ, the force applied to the sensing element can be obtained as:

$$F = K* \Delta \quad (5)$$

where K is the stiffness of the corresponding sensing element (the slope of data in Figure 4(a)). Hence by substituting (4) into (5), the force can be calculated as:

$$F = (K/K_v)*(V-V_0) \quad (6)$$

Table 1. Calibration results for all sensing elements

Sensor	*K (N/mm)*	*Maximum deflection (μm)*	*Max. support force (N)*	*Maximum signal change (V)*	*K_v (V/mm)*	*K_v/K (V/N)*	*V_0 (V)*	*Flexing arm length(mm)*
1	40.12	74.3	2.96	0.55	-7.3	-0.182	-1.01	4
2	11.57	118.9	1.41	0.59	-4.9	-0.425	0.08	7
3	14.91	103.7	1.55	0.37	-3.6	-0.239	-0.08	6
4	5.78	143.1	0.85	0.53	-3.8	-0.652	-2.14	8
6	7.35	135.2	1.04	0.63	-4.6	-0.623	0.10	8
7	15.25	108.7	1.78	0.40	-3.7	-0.241	-1.47	5
8	80.38	50.6	4.33	0.47	-9.0	-0.112	0.20	4
9	15.05	105.3	1.64	0.63	-6.0	-0.401	0.05	5
10	9.05	123.5	1.20	0.45	-3.7	-0.408	-0.33	7

Maejo Int. J. Sci. Technol. **2014**, *8*(02), 165-180

The stiffness provided by the sensing elements (*K* column in Table 1) shows a stiffness ratio of 13.9 between the stiffest sensing element (element 8) and the softest (element 4). This was measured while the arm length of the sensing elements was varied from 4 to 8 mm for the stiffest and softest elements respectively. Thus, by changing the length of measuring arm, the stiffness of the sensing elements could be easily tuned. Three of the nine functioning sensing elements (elements 3, 7 and 9) had very close stiffness values within 2.3%. To avoid redundancy in results, one of them was picked to represent the others, making a total of 7 distinct sensing elements. As the maximum deflection (column 3) shows, most of the sensing elements experienced deflections of more than 100 μm. It was assumed that such level of deflection should be sufficient in calibrating the sensing elements. The maximum changes in signal for all the sensing elements, irrespective of the applied deflection and force, showed readings of the same order.

The sensitivity of the sensing elements is one of the key factors for their performance. In this study two different sensitivity parameters are considered: sensitivity of signal output of the sensing elements with respect to force and to deflection. The K_v (V/mm) column in Table 1 lists the former and the K_v/K (V/N) column, the latter. The highest sensitivity of signal to deflection belongs to the stiffest element(s) and the lowest sensitivity, to the softest element(s). During the grasping of tissues, the pressure in the tissue-grasper interface is directly translated as the force applied to the sensing elements. So the sensitivity of signal to applied force is more crucial for the overall performance of the tactile sensors (column K_v/K). Comparing the K_v/K ratio of different sensing elements, it can be observed that the softer sensing element has a higher signal-to-force sensitivity than does the stiffer elements. For example, the softest sensing element's sensitivity of -0.652 V/N was recorded while for the stiffest sensing element it was -0.112 V/N. Contrary to this trend, the K_v sensitivity parameter decreases while moving from the stiffest sensing element to the softest one.

Tissue Phantom Test: Specimen and Test Set-up

Our search for suitable test samples for tissue phantom as applicable to the present study was mainly based upon two criteria: 1) the elasticity/stiffness needs to be demonstrated over a wide range in order to evaluate the stiffness sensing, and 2) the material should be continuum compliant so that multiple-measurement data can be obtained for discerning generic trends over a relevant range of forces and resilience. Various gel-based, soft tissue phantoms were tried initially for their suitability. However, the soft gels tended to break under multi-point force application as desired in this study (within the force/stiffness range as deduced from the literature). Further experiments were carried out using animal tissues acquired directly from wet markets. The large variation of the data observed among different samples as well as sections of the same sample, however, precluded their use as standard test samples at this stage, when the emphasis was more on testing the desired parametric characteristics of the fabricated sensors. The high variation in the test environment could lead to inconclusive outcomes on sensing feasibility over the desired stiffness range. Thus, rubber samples were chosen to resemble a continuum-compliant medium with the main emphasis on their stiffness characteristics that can provide a reasonably acceptable range for the present application. Thereby, a range of commercially available rubber samples with varied stiffness values were used for simulating biological samples. The stiffness tests on these samples were conducted in the laboratory and those with stiffness values comparable to those of the softer sensing elements in Table 1 were selected for validation purpose. However, we understand that the magnitude of stiffness for rubber samples is higher than that for biological tissues.

Maejo Int. J. Sci. Technol. **2014**, *8*(02), 165-180

A mechanical set-up as shown in Figure 5 was arranged for obtaining the stiffness of rubber samples. The individual samples were positioned in the clamping area of a wheeled cart as shown. Vacuum clamping created by a vacuum pump and pneumatic hose was used to hold the sample on the cart. The cart itself was situated on the base plate through four ball-bearings. In this manner, no horizontal force could be created at the interface between the macro-tactile array and rubber sample. Only vertical forces were then applied at the interface of the force sensor and rubber sample. The force sensor was displaced towards the rubber sample in increments of 50 µm and to a maximum distance of 300 µm. For a given sensor's contact area of the size adopted in this study, such magnitude was considered to be sufficient [23]. The contact force was then measured at each step, thereby generating the force-deflection relationship for all the samples. The measuring apparatus and the sensing elements had the same contact area of 2×3 mm^2.

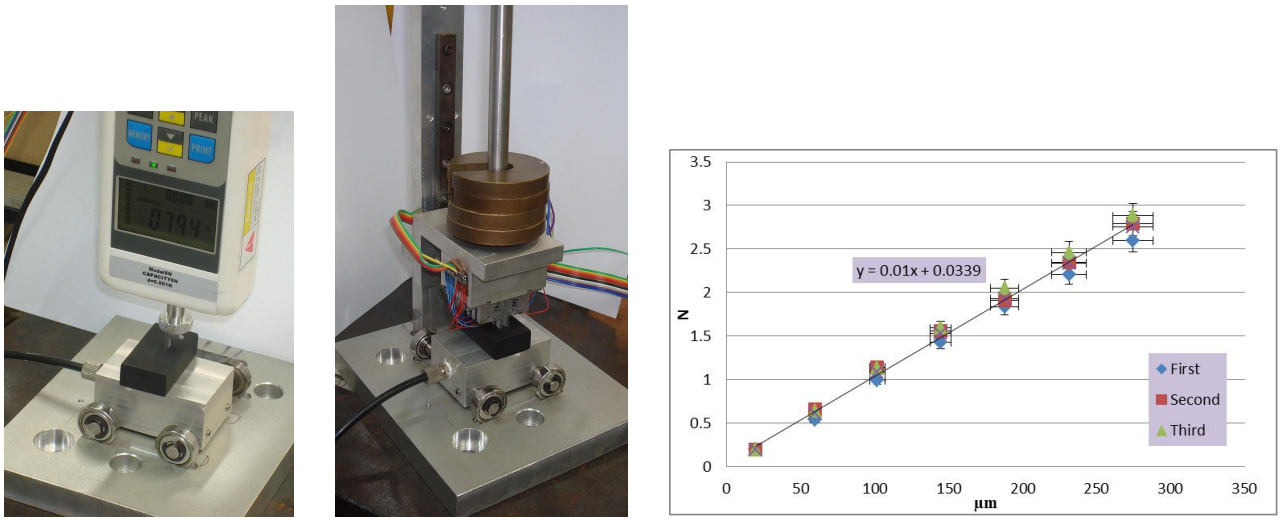

(a) (b) (c)

Figure 5. (a) Mechanical set-up for measuring the stiffness of rubber samples; (b) Evaluating stiffness of rubber samples by macro-tactile array; (c) Force-deflection relationship for one of the rubber samples

Fifteen test samples were used and measurement of the force-deflection relationship for each sample under a quasi-static condition as described above was repeated three times and the averaged readings were plotted to study the force-deflection relationship as shown in Figure 5(c). It was found that the samples have a linear force-deflection relationship and their linearity error varies in the range of 0.72-1.9%. Eight out of fifteen samples were found to have distinct stiffness values. The sample stiffness varies in the range of 2.34-10.01 N/mm, resulting in the stiffness ratio of the stiffest sample to the softest one being ~4.28. This ratio provides an acceptable range of variation in stiffness value of the samples.

Stiffness Evaluation Using Macro-Tactile Array

In Table 1 the stiffness of the tactile sensing elements varies between 5.78-80.384 N/mm. Comparing this range with the one provided by the rubber samples shows that the ratio of stiffness for the stiffest sensing element (highest K_m) when in contact with the softest rubber sample is 40.12/2.34=17.14, while the same ratio for the softest sensing element to the stiffest rubber sample is 5.78/10.01= 0.577. This wide range of ratios of 0.577-17.14 from combinations of the sensing

Maejo Int. J. Sci. Technol. **2014**, *8*(02), 165-180

elements and rubber samples exhibits a stiffness range sufficient for all biological tissues, thus verifying the validity of the sensing concept proposed in this study.

The stiffness of rubber samples was evaluated by the macro-tactile array and was compared with the measurements obtained using a commercial force sensor. For this purpose another mechanical set-up was designed and fabricated as shown in Figure 5(b), where the macro-tactile array was fixed on a linear axis that could be displaced vertically while the rubber sample was fixed on a wheeled cart. Standard weights of 100 g each were used to implement the vertical grasping force in the macro-tactile array and rubber sample interface. These weights were pre-calibrated with a standard commercial force sensor. Each of the eight samples was tested by placing them on the central part of the cart's top surface and was clamped firmly by suction power of the vacuum pump. Next, the macro-tactile probe, installed on the vertical axis, was gently brought in contact with the rubber sample.

The first value of the grasping force between the macro-sensor array and the rubber sample was equal to the weight of the vertical axis itself. This weight included that of the linear carrier, the vertical bar and the macro-tactile array, which all together added up to 3.235 N. At first, the data were collected when there was no loading between the macro-tactile array and rubber sample, i.e. under zero grasping force. In the next loading steps, 100-g weights were added one at a time. The data acquisition programme in the Lab-View was set to collect 10 data samples for every measurement step. The average value, as representative for each measurement attempt, was calculated and saved. Figure 6 shows a typical set of graphs which illustrate the data collected for eight rubber samples during the loading of reference sample with a stiffness of 3.85 N/mm.

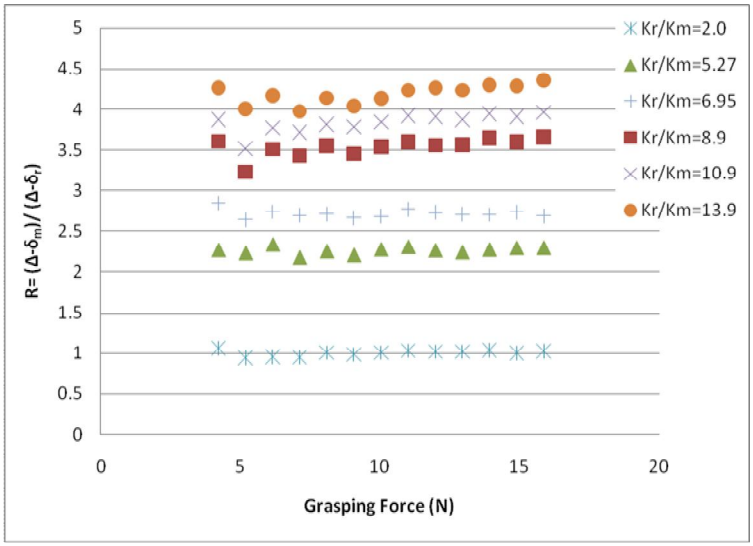

Figure 6. The measuring element deflection (Δ-δ_m) to reference element deflection (Δ-δ_r) ratio, R, for different stiffness combinations of K_r/K_m in the case of rubber sample with 3.85 N/mm of stiffness

The deflection readings of all sensing elements, excluding the stiffest one, were divided by the deflection of the stiffest sensing element to obtain these graphs. In our formulation, K_r is used to represent the stiffness of the stiffest element (the reference element) and K_m is used to represent the stiffness of the rest of the elements (the measuring element). Thus, Figure 6 is an illustration of the ratio of deflection of the measuring elements, Δ-δ_m, to the deflection of the stiffest element, Δ-δ_r. The

horizontal axis is the applied grasping force in Newton and the vertical axis represents the deflection ratio, $R = (\Delta-\delta_m)/(\Delta-\delta_r)$. Since K_r is greater than K_m, the ratio R is always larger than 1.0. As Figure 6 shows, in the case of all K_r/K_m combinations, the R ratio for different values of grasping force mostly remains constant, which implies that the deflection ratio of the tactile sensor array, R, is independent of the change in the grasping force present at the interface of the macro-tactile sensor and the rubber sample.

Validation and Overall Performance of Tactile Array

As eight rubber samples with different stiffness values were chosen to mimic biological tissues with different stiffness, eight different graphs were obtained, of which Figure 6 is a member. A more detailed (discrete points) and conclusive information can be presented in a tabular form as represented in Table 2. Based on such experimental information, the performance of the macro-tactile array in sensing object stiffness not only can be evaluated, but it can also be used to validate the sensing concept itself. As the ratio R mainly remains constant for different values of grasping force, each of these graphs can be viewed as six average values for R. By sorting R values for the softest rubber sample to the stiffest one, a generic trend for variability in R can be obtained.

Table 2. The readings of macro-tactile sensors during the grasping of rubber samples with different stiffness (K_r= 80.38 N/mm)

K_m (N/mm)	K_r/K_m		K_{obj} (N/mm)							
			10.01	7.26	6.28	5.41	4.51	3.85	3.57	2.34
40.12	2.004	K_m/K_{obj}	4.083	5.541	6.470	7.412	9.008	10.610	11.226	17.085
		R	0.977	0.840	0.830	0.822	1.002	1.004	0.942	1.416
15.25	5.270	K_m/K_{obj}	1.552	2.107	2.460	2.818	3.425	4.033	4.268	6.495
		R	1.729	1.816	2.001	2.002	2.174	2.283	2.186	2.461
11.57	6.950	K_m/K_{obj}	1.177	1.597	1.865	2.137	2.597	3.059	3.236	4.926
		R	2.134	2.402	2.410	2.320	2.787	2.757	2.852	3.770
9.05	8.884	K_m/K_{obj}	0.921	1.249	1.459	1.672	2.0312	2.393	2.532	3.853
		R	2.938	3.002	2.993	3.253	3.601	3.536	3.828	4.523
7.35	10.933	K_m/K_{obj}	0.748	1.015	1.186	1.358	1.651	1.944	2.057	3.131
		R	2.827	3.119	3.257	3.407	3.729	4.064	4.225	4.779
5.78	13.905	K_m/K_{obj}	0.588	0.798	0.932	1.068	1.298	1.529	1.617	2.462
		R	3.142	3.324	3.480	3.534	3.994	4.186	4.293	5.451

As the stiffest sensing element in the macro-sensor array was the element no. 8 with 80.38 N/mm of stiffness (Table1), this sensing element was considered as the reference sensing element and the other eight elements softer than this were considered the measuring sensors. As stated earlier, the stiffness of the reference sensing element was represented by K_r and the stiffness of the measuring

Maejo Int. J. Sci. Technol. **2014**, *8*(02), 165-180

elements, by K_m. The values of K_m are listed as the first column in Table 2 and the second column shows all the available combinations of reference versus measuring sensors as K_r/K_m ratios in ascending order. Eight possible combinations for K_r and K_m were expected as there were nine functioning sensors in the sensing array. However, as mentioned earlier, the sensing elements no. 3, 7 and 9 having almost the same stiffness, element no. 7 was chosen to represent others. In this way the total number of K_r/K_m ratios was reduced to six.

The R values versus K_m/K_{obj} variation are listed in Table 2 for a given K_r/K_m combination of the reference element and the measuring element. Thus, this Table can be used for performance analysis of the macro-tactile array. Figure 7 represents K_m/K_{obj} with respect to the corresponding R ratio and each of the six trend lines belongs to one of the K_r/K_m values in Table 2. It can be seen that any increase in K_m/K_{obj} (moving from stiffer samples to softer ones) leads to an increase in R for all the given K_r/K_m combinations in the tactile array. Smaller K_r/K_m ratios (in the vicinity of 2.0) were ignored since they would have insignificant stiffness sensitivity in the evaluation of object stiffness. For K_r/K_m= 5.27 and larger, this sensitivity improves remarkably.

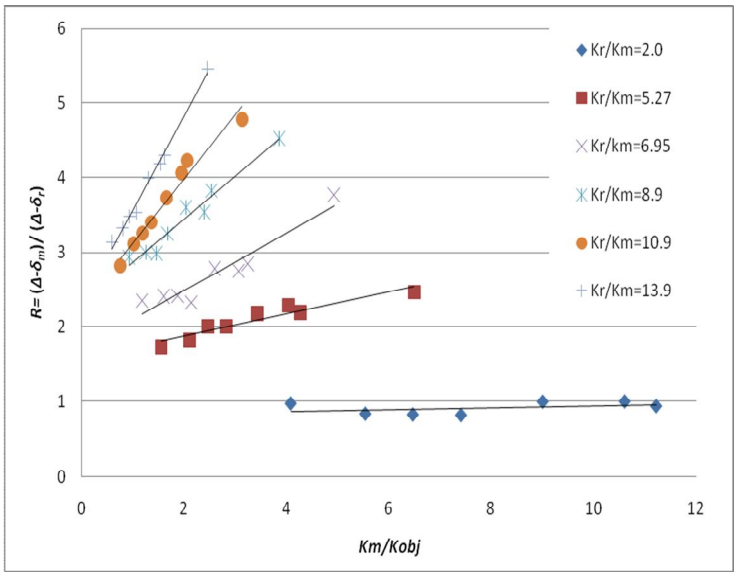

Figure 7. Performance of macro-tactile sensor in grasping rubber samples with different stiffness

For further performance evaluation, both the deflection range and the output signal range in the reference element were monitored. The reference element, being the stiffest, was expected to undergo the lowest deflection among all the sensing elements. Furthermore, the reference element showed the lowest value for K_v/K ratio (Table 1), the sensitivity of signal with respect to the force applied in the sensing element. The maximum signal change for the reference element in grasping the rubber sample was in the range of 0.06-0.14 V, which indicated a deflection range of 28.6-37.2 µm in the reference element. A signal change of up to 0.61V and a deflection of 141.9 µm were experienced in some of the softer elements.

CONCLUSIONS

In an attempt towards the safe handling and grasping of tissues during MIS, a spring-based stiffness sensor is proposed in this paper. The sensor is an array of force sensors made up of two sets of force sensing elements with different stiffness. As a result, both stiffness and force can be

Maejo Int. J. Sci. Technol. **2014**, *8*(02), 165-180

measured simultaneously. A lumped model is used to describe the sensor performance. This model includes the stiffness of two force sensing elements: K_r for the reference and K_m for the measuring force sensing elements. The stiffness, K_{obj}, refers to the object with which the sensing elements come in contact. The ratio of deflection of the measuring sensing element to that of the reference sensing element is defined as the output for the stiffness sensing unit. A lumped model correlates this ratio (K_r and K_m) with K_{obj}. It was found that a higher stiffness difference between the force sensing elements (i.e. higher K_r/K_m) provides a higher sensitivity for the evaluation of object stiffness. Furthermore, larger K_m/K_{obj} values can help to improve the sensitivity of sensing the object stiffness.

A macro-sensor array is fabricated as a benchmark to validate the sensor design concept. Sensing elements with different stiffness are realised by providing different measuring arms in a flexural sensing mechanism. Rubber samples were used to mimic biological tissues during the experiments with stiffness in the range of 2.34-10.01 N/mm. As a result, a wide range of sensor-rubber stiffness combinations was available during the experiments. Such a wide range makes it possible to validate the sensing concept. It was shown that the deflection ratio of the tactile sensor array, R, is independent of changes in the grasping force but when the same K_r/K_m comes in contact with rubber samples with different stiffness and K_m/K_{obj} is subjected to change, the R ratio varies linearly. Thus, it can be concluded that the proposed design concept is capable of evaluating the stiffness of objects. The experimental results suggest that it is favourable to have a high K_r/K_m to improve the sensitivity of the stiffness evaluation while sufficient signal readings and deflection of the reference sensing elements are secured. Otherwise, the results regarding the evaluation of object stiffness might be misleading. So the ratio of K_r/K_m for fabrication of the MEMS should be optimised, which is proposed to be ~10 based on the results of our experiments.

REFERENCES

1. P. Puangmali, K. Althoefer, L. D. Seneviratne, D. Murphy and P. Dasgupta, "State-of-the-art in force and tactile sensing for minimally invasive surgery", *IEEE Sensors J.*, **2008**, *8*, 371-381.
2. P. Valdastri, K. Harada, A. Menciassi, L. Beccai, C. Stefanini, M. Fujie and P. Dario, "Integration of a miniaturised triaxial force sensor in a minimally invasive surgical tool", *IEEE Trans. Biomed. Eng.*, **2006**, *53*, 2397-2400.
3. S. Omata and Y. Terunuma, "New tactile sensor like the human hand and its applications", *Sensors Actuat. A: Phys.*, **1992**, *35*, 9-15.
4. Y. Murayama, C. E. Constantinou and S. Omata, "Development of tactile mapping system for the stiffness characterization of tissue slice using novel tactile sensing technology", *Sensors Actuat. A: Phys.*, **2005**, *120*, 543-549.
5. Y. Murayama, M. Haruta, Y. Hatakeyama, T. Shiina, H. Sakuma, S. Takenoshita, S. Omata and C. E. Constantinou, "Development of a new instrument for examination of stiffness in the breast using haptic sensor technology", *Sensors Actuat. A: Phys.*, **2008**, *143*, 430-438.
6. T. Hemsel, R. Stroop, D. Oliva Uribe and J. Wallaschek, "Resonant vibrating sensors for tactile tissue differentiation", *J. Sound Vibrat.*, **2007**, *308*, 441-446.
7. N. Sakai, M. Tatsuta, H. Yano, H. Iishi and S. Ishiguro, "Diagnosis of the extent of gastric cancers by a new endoscopic ultrasonic tactile sensor", *Gastrointest. Endosc.*, **2000**, *51*, 69-73.

Maejo Int. J. Sci. Technol. **2014**, *8*(02), 165-180

8. S. Omata, Y. Murayama and C. E. Constantinou, "Real time robotic tactile sensor system for the determination of the physical properties of biomaterials", *Sensors Actuat. A: Phys.*, **2004**, *112*, 278-285.
9. N. Kattavenos, B. Lawrenson, T. G. Frank, M. S. Pridham, R. P. Keatch and A. Cuschieri, "Force-sensitive tactile sensor for minimal access surgery", *Minim. Invasive Ther. Allied Technol.*, **2004**, *13*, 42-46.
10. S. Schostek, C. N. Ho, D. Kalanovic and M. O. Schurr, "Artificial tactile sensing in minimally invasive surgery – a new technical approach", *Minim. Invasive Ther. Allied Technol.*, **2006**, *15*, 296-304.
11. H. Takao, M. Yawata, K. Sawada and M. Ishida, "A multifunctional integrated silicon tactile imager with arrays of strain and temperature sensors on single crystal silicon diaphragm", *Sensors Actuat. A: Phys.*, **2010**, *160*, 69-77.
12. M. Shikida, T. Shimizu, K. Sato and K. Itoigawa, "Active tactile sensor for detecting contact force and hardness of an object", *Sensors Actuat. A: Phys.*, **2003**, *103*, 213-218.
13. J. Engel, J. Chen, Z. Fan and C. Liu, "Polymer micromachined multimodal tactile sensors", *Sensors Actuat. A: Phys.*, **2005**, *117*, 50-61.
14. J. Engel, J. Chen and C. Liu, "Development of polyimide flexible tactile sensor skin", *J. Micromech. Microeng.*, **2003**, *13*, 359-366.
15. J. Dargahi, S. Najarian and B. Liu, "Sensitivity analysis of a novel tactile probe for measurement of tissue softness with applications in biomedical robotics", *J. Mater. Process. Technol.*, **2007**, *183*, 176-182.
16. P. Peng, A. S. Sezen, R. Rajamani and A. G. Erdman, "Novel MEMS stiffness sensor for force and elasticity measurements", *Sensors Actuat. A: Phys.*, **2010**, *158*, 10-17.
17. W. L. Jin and C. D. Mote Jr, "Development and calibration of a sub-millimeter three-component force sensor", *Sensors Actuat. A: Phys.*, **1998**, *65*, 89-94.
18. M. Adam, T. Mohacsy, P. Jonas, C. Dücso, E. Vazsonyi and I. Barsony, "CMOS integrated tactile sensor array by porous Si bulk micromachining", *Sensors Actuat. A: Phys.*, **2008**, *142*, 192-195.
19. M. Adam, E. Vazsonyi, I. Barsony, G. Vesarhelyi and C. Dücso, "Three dimensional single crystalline force sensor by porous Si micromachining", *Proc. IEEE Sensors*, **2004**, *1*, 501-504.
20. G. Vasarhelyi, M. Adam, E. Vazsonyi, Z. Vizvary, A. Kis, I. Barsony and C. Dücso, "Characterization of an integrable single-crystalline 3-D tactile sensor", *IEEE Sensors J.*, **2006**, *6*, 928-934.
21. R. S. Dahiya, G. Metta, M. Valle and G. Sandini, "Tactile sensing—from humans to humanoids", *IEEE Trans. Robotics*, **2010**, *26*, 1-20.
22. R. S. Dahiya, D. Cattin, A. Adami, C. Collini, L. Barboni, M. Valle, L. Lorenzelli, R. Oboe, G. Metta and F. Brunetti, "Towards tactile sensing system on chip for robotic applications", *IEEE Sensors J.*, **2011**, *11*, 3216-3226.
23. M. E. Rentschler, J. Dumpert, S. R. Platt, K. Iagnemma, D. Oleynikov and S. M. Farritor, "Modeling, analysis, and experimental study of in vivo wheeled robotic mobility", *IEEE Trans. Robotics*, **2006**, *22*, 308-321.

Maejo Int. J. Sci. Technol. **2014**, *8*(02), 165-180

24. S. P. Abbas, S. Chauhan, S. J. Phee and G. K. Lau, "Real-time, non-vision sensory feedback during minimally invasive surgery", Proceedings of IEEE Region 10 Conference (Tencon 2009), **2009**, Singapore, pp.1-6.